Optimal network configuration for maximal coherence resonance in excitable systems

Marko Gosak,[1,*] Dean Korošak,[2,3] and Marko Marhl[1]
[1]*Department of Physics, Faculty of Natural Sciences and Mathematics, University of Maribor, Koroška cesta 160, SI-2000 Maribor, Slovenia*
[2]*Faculty of Civil Engineering, University of Maribor, Smetanova ulica 17, SI-2000 Maribor, Slovenia*
[3]*Institute of Physiology, Faculty of Medicine, University of Maribor, Slomškov trg 15, SI-2000 Maribor, Slovenia*
(Received 2 December 2009; revised manuscript received 22 February 2010; published 18 May 2010)

We analyze the coherence resonance phenomenon in an ensemble of noise-driven excitable neurons giving special attention to the role of the interaction topology. The neural architecture is modeled using a spatially embedded network in which we can tune the network organization between scale-free-like with dominating long-range connections and a network with mostly adjacent neurons connected. We found that besides an optimal noise intensity, also an optimal network configuration exists at which the largest average coherence of noise-induced spikes is achieved. Furthermore, we show that long- as well as short-range interactions between neurons should exist in order to achieve the optimal response of the neuronal network.

DOI: 10.1103/PhysRevE.81.056104 PACS number(s): 89.75.Hc, 05.40.−a, 87.18.Sn

I. INTRODUCTION

It is well known that noise can act as an ordering agent in several nonlinear systems. Perhaps the most famous phenomenon related to this apparently paradoxical fact is stochastic resonance, where the response of a weakly driven stochastic nonlinear system exhibits a resonancelike dependence on the noise intensity (for review, see [1]). Interestingly, constructive effects of noise can also be observed in systems without weak external inputs, whereby the established term describing this phenomenon is coherence resonance [2,3]. A particularly lively subject appears to be the study of noise-induced effects in excitable systems [4], since excitability has been recognized as a fundamental property of several biological and artificial systems [5]. Perhaps the most striking examples concern neuronal systems [6], although several other examples range from cardiac tissue [7] and chemical reactions [8] to laser optics [9] and aquatic ecosystems [10].

While primal investigations of stochastic and coherence resonances have scrutinized mainly systems with relatively small numbers of degrees of freedom, the scope has been shifting to coupled and spatially extended systems with many degrees of freedom, where numerous interesting contributions regarding collective noise-induced dynamic behavior have been reported (for review, see [11]). Here, we would like to highlight the quite recent work of Tessone *et al.* [12], who showed that intrinsic diversity, i.e., static disorder, can also provoke a resonantly enhanced collective behavior, where the response of the system exhibits a clear maximum with the variation of inherent variability. Their findings were recognized to play an important role in several other setups ranging from soft-matter systems [13] to biological signaling pathways [14], whereby special attention has been devoted to ensembles of neural elements [15].

In the past, the majority of scientific research dealing with spatially extended systems was devoted to the study of the dynamics on regular networks. However, recently, the focus has been shifting toward ensembles characterized with complex interaction topologies, as constituted by small-world or scale-free networks [16]. Such networks appear to be excellent for modeling of interactions among units in complex systems, since many natural, social, and technological systems can be regarded as complex networks, in which vertices represent interacting units and the edges signify interactions among them. In particular, small-world and scale-free network properties have been identified in several real-world networks such as the world-wide web, scientific collaboration, and other social networks as well as in biological networks [17]. Furthermore, many real networks are embedded in metric space and the connectivity is also a function of the Euclidean distance between the vertices [18]. The most prominent examples of such complex networks are the internet, mobile communication, traffic networks, and power grids. Most remarkably and immediately related to the present study are the recent studies which have revealed that the same general principles in the structural and functional organizations of complex networks are present in the nervous system [19,20]. Those features were found on microscopic level, considering individual neurons, as well as on macroscopic level, in the context of gross neural connectivity.

Recently, stochastic and coherence resonances have been intensively studied on complex networks in various situations [21–23]. In particular, studies incorporating small-world network models in general point out an enhanced response and a greater synchronization due to the added shortcut links [21]. Furthermore, similar investigations on scale-free networks also emphasize advantages of complex interaction topologies [22,23].

In contrast to these previous studies on small-world and scale-free networks, we are trying to find out the best network configuration at which the noise-induced oscillations are the most regular without choosing any specific network configuration. To this purpose, we analyze the coherence resonance phenomenon in a noise-driven excitable system by embedding individual units in Euclidean space. In particular, we construct a network representation of the neural architecture, where the vertices are excitable neurons and the links

*Corresponding author. FAX: +386 2 2518180; marko.gosak@uni-mb.si

model interactions among them. Development of our network model is based on the vertex fitness network model [24,25] and the spatially embedded vertex fitness network model [26]. Accordingly, a fitness value is assigned to each element of the network and vertices are connected with the probability depending on the vertex fitness and their spatial localization. Notably, variability of vertex fitness values is a consequence of diversity of neuron cells, which is realized by distributing the thresholds values for large-amplitude firing of individual neurons. Moreover, a control parameter is present in the model which signifies the nature of the network. In particular, by modifying the parameter, the network topology can smoothly be altered between a scale-free-like network with dominating long-range connections originating from highly connected nodes and a random geometric network where mostly adjacent neurons are connected. In this study, in which we do not prejudice any network configuration of the neuronal architecture, we show that for different distributions of excitability, the optimal network topology is always between a scale-free-like network organization and a strong geometric regime. Our results thus indicate that long- as well as short-range interactions between neurons should exist in order to ensure an optimal response of the neuronal network.

II. MATHEMATICAL MODEL AND SETUP

One of the most commonly used models of excitable oscillators is the famous Fitzhugh-Nagumo system [27], which has been derived from the Hodgkin-Huxley model describing the excitable dynamics of electrical signal transmission along neuron axons [28], but is due to its relatively simplicity nowadays utilized for the description of various situations exhibiting excitability. In the present study, we also utilize the Fitzhugh-Nagumo equations for managing the dynamics of individual units. The model along with the additive noise and the coupling term takes the following form:

$$\kappa\frac{du_i}{dt} = u_i(1-u_i)\left(u_i - \frac{v_i+b}{a_i}\right) + D\sum_j \varepsilon_{ij}(u_j-u_i) + \sigma\xi_i, \tag{1}$$

$$\frac{dv_i}{dt} = u_i - v_i, \tag{2}$$

where $u_i(t)$ and $v_i(t)$ are dimensionless variables representing the membrane potential and the time-dependent conductance of potassium channels of the ith unit, respectively. Parameter $\kappa \ll 1$ guarantees that the dynamics of u_i is much faster than that of v_i and σ signifies the intensity of additive Gaussian white noise ξ_i with zero mean and unit variance. Parameters b and a determinate the excitable dynamics, where the latter is assumed to follow a power-law distribution

$$P(a) \sim a^{-\beta}. \tag{3}$$

In particular, values of a_i are assigned deterministically as follows [26]:

$$a_i = (i/N)^{1/(1-\beta)}, \tag{4}$$

where $i=1,2,\ldots,N$ and N signifies the number of units. Then, we bound the given values a_i so that they are confined within the interval $a_i \in [0.51, 0.99]$ for any values of β, whereby the characteristics of the distribution remains unchanged. In this manner, the dynamics of each oscillator is governed by a single excitable steady state $u_i=v_i=0$. When perturbations of the excitable steady state exceed the threshold, the system is set into the firing state, which is characterized by large-amplitude spikes. Heterogeneity of values a_i introduces diversity of the threshold values for large-amplitude firings, whereby the thresholds decrease with increasing values of a_i.

The sum in Eq. (1) signifies the coupling and it runs over all units, whereby $\varepsilon_{ij}=1$ if the cell i is coupled to cell j, while otherwise $\varepsilon_{ij}=0$. D is the coupling constant. The network connectivity was calculated as follows [26]:

$$\Pi_{i\to j} \sim \frac{a_i a_j}{(l_{i,j})^{\delta}}, \tag{5}$$

where $l_{i,j}$ signifies the Euclidean distance between ith and jth cell and δ is a model parameter that controls the range of interaction between the cells, with $\delta \leq 1$ for long-range interactions and $\delta \gg 1$ for short-range interactions. Thus, the ith and jth cells are connected if the connectivity exceeds the threshold value $\Pi_{i\to j} > \Theta$. Given a fixed set of N cells, we can set the number of links (or mean vertex degree $\langle k \rangle$) in the network by choosing the appropriate Θ. The model given by Eq. (5) is similar to the probability function employed by Morita [26], where, for simplicity reasons, the distance $l_{i,j}$ was defined by the $L_{\max}$ norm, while in our calculations, the usual L_2 norm is used. Furthermore, in contrast to the model in Ref. [26], we did not apply any boundary conditions. Spatial localization of individual cells was determined by randomly distributing the vertices on a plane and no correlations between the position and values of a_i were assumed. We show in the upper row of Fig. 1 some characteristic examples of network generation for different δ. Clearly, for $\delta=0.5$, long-range connections are dominating in the network mostly originating from a few well-connected vertices, i.e., hubs. Here, the majority of the units are connected exclusively to some of those highly connected vertices, which have the largest values of a_i. On the other hand, for $\delta=5$, the distance between the units is the key constraint that defines the topology of the network, so that in general, only adjacent units are connected. For intermediate values of δ, long-range as well as short-range interactions can be found. In order to quantify the network properties, we calculated the corresponding degree distributions. As shown in the lower row of Fig. 1, the degree distribution for the network with $\delta=0.5$ is highly inhomogeneous, indicating a scale-free character of the network, and for $\delta=5$, the degree distribution obeys a Poisson distribution, hallmark of random graphs. For intermediate values of δ, for example, $\delta=1.5$, the degree distribution follows a power law at least in a certain extent. We can observe that there are still some well-connected hubs. However, on account of connections that are present also between neighboring units, the degree of the most connected

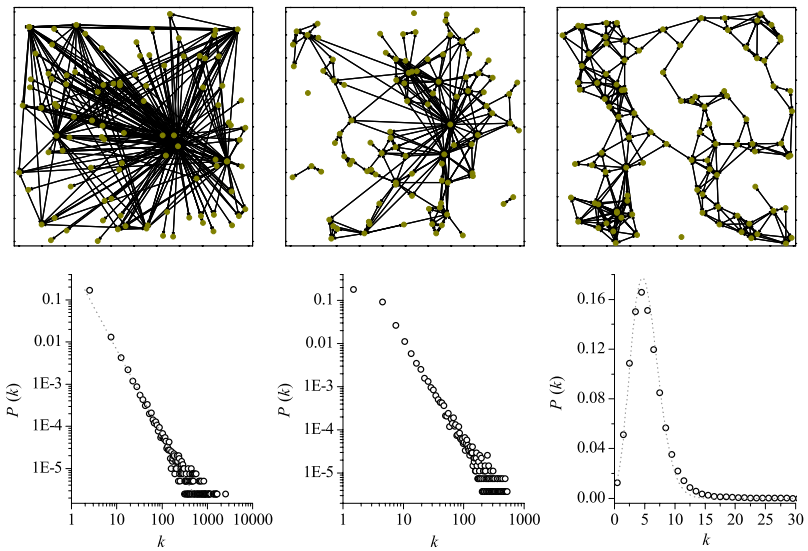

FIG. 1. (Color online) Characteristic network representations of the neural architecture (upper row) for $\delta=0.5$ (left panel), $\delta=1.5$ (middle panel), and $\delta=5$ (right panel) and the corresponding degree distributions (lower row). In both cases, the mean degree was set to $\langle k\rangle=5$ and the scaling exponent was $\beta=2.5$. The number of units in network representations is $N=100$, whereas the calculation of the degree distribution was performed for $N=5000$ nodes and averaged over ten independent network generations.

vertices is in this case considerably smaller as it is in the case with $\delta=0.5$.

It should be emphasized that the power-law distribution of a_i is not crucial, but also others, e.g., uniform or Gaussian distribution, could be used with values confined in the same interval. With the other distributions, qualitatively similar networks appear in dependence on δ, e.g., for δ close to 0, we get a network with only few hubs, which are connected with the majority of the nodes via long-range links, but in this case, the degree distribution does not exactly follow the power law. As it was shown by Servedio *et al.* [25], a scale-free network can be produced by arbitrary distributions of vertex fitnesses, but in this case one has to find a suitable linking probability function, which is in general different from those used in the present study [Eq. (5)], even at $\delta=0$.

Due to the inhomogeneous distribution of the thresholds for large-amplitude firings, the dynamics of the network is governed by a pacemaker-like mechanism. Namely, units with lower thresholds are triggered earlier and thus imply their rhythm to other units of the network. As a result, an interesting interplay between noise intensity, coupling properties, and the distribution of a_i is observed. In particular, we are especially focused on the impact of network configuration on the quality of the noise-induced global response. In order to quantify the coherence of noise-induced firing at different noise intensities and for different network configurations, we calculate the normalized autocorrelation function of $u_i(t)$,

$$C_i(\tau)=\frac{\langle \tilde{u}_i(t)\tilde{u}_i(t+\tau)\rangle}{\langle \tilde{u}_i^2(t)\rangle}, \tag{6}$$

where $\tilde{u}_i=u_i-\langle u_i\rangle$. Afterwards, we signify the regularity of firings by calculating the correlation time T_i according to the formal equation for each of the units

$$T_i=\int C_i^2(t)dt, \tag{7}$$

which is a suitable and commonly used measure for the regularity of the excitations [3]. In particular, larger values of T_i correspond to a greater coherence of noise-induced spikes. In order to evaluate the response of the entire network with a single quantity, we introduce $\bar{T}$, the average T_i of all units, defined as $\bar{T}=N^{-1}\Sigma_{i=1}^{N}T_i$. Importantly, the final average correlation time $\bar{T}$ presented in the figures was obtained by averaging over 50 independent realizations in order to reduce statistical fluctuations originating from the stochastic dynamics and from randomness incorporated in network generations. System parameter values used throughout the study were $b=0.01$, $\kappa=0.02$, $D=0.5$, $\langle k\rangle=5$, and $N=100$.

III. RESULTS

In what follows, we will present the noise-induced response of the units in dependence on the network topology and on the noise intensity. For this purpose, we calculated $\bar{T}$ for different noise intensities σ and for different network configurations δ. The color-contour plot in the left panel of Fig. 2 features the results. It can be observed nicely that besides optimal noise intensity, also a greatest possible network configuration exists at which the noise-induced firing of the whole network is most regular. Furthermore, the cross section presented in the right panel of Fig. 2 showing $\bar{T}$ in dependence on δ at optimal noise strength additionally corroborates the resonant response due to the change in topology.

To gain more insight into the observed phenomenon, we show in Fig. 3 responses of individual units T_i for three characteristic values of δ. It can be noticed that in case where long-range connections are dominating in the network and the degree distribution is a scale-free-like ($\delta=0.5$), values of T_i decrease quite quickly with increasing i. At this point, it should be emphasized once again that values of a_i are also decreasing with increasing i, as given by Eq. (3). However, in the middle panel of Fig. 3, where the responses at $\delta=1.5$ are shown, we can observe that in comparison to the case where $\delta=0.5$, values of T_i decrease slower, so that a larger portion of the units exhibit larger values of T_i. Accordingly, in this case, a greater collective response reflected by $\bar{T}$ is

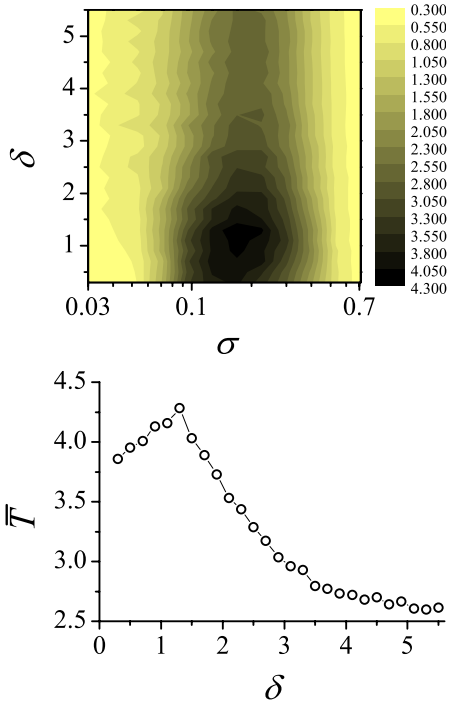

FIG. 2. (Color online) Color-coded values of $\bar{T}$ in dependence on σ and δ (upper panel) and the cross section of the color map at optimal noise intensity σ=0.17 (lower panel) for the scaling exponent β=2.5.

noticed, as already recognized in Fig. 2. Finally, in the case where mostly neighboring units are connected and the degree distribution obeys a Poisson distribution (δ=5), the coherence of individual units does not significantly depend on i and values T_i. The units with the highest excitability (i <10) are quite lower as in the former two cases, so that consequently values of $\bar{T}$ are lower too. These results clearly indicate that an optimal response of neural network is achieved in the intermediate regime between a network with a few very well connected hubs and a random geometric network. Apparently, very big differences in connectivity between individual units in networks with dominating long-

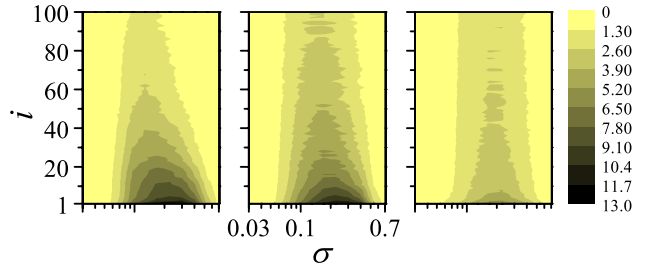

FIG. 3. (Color online) Resonant responses of individual units T_i in dependence on σ for different network configurations: δ=0.5 (left panel), δ=1.5 (middle panel) and δ=5 (right panel). The scaling exponent β is the same as in Fig. 2.

range connections (see left column in Fig. 1) result in a less coherent collective response. It seems that even though neurons with the lowest-firing thresholds have widespread connections almost over the whole network, the best coherence in this case cannot be achieved due to the discrepancy in the node degree. On the other hand, in a network with mainly short-range interactions, there are no distinctive differences in connectivity so that the most excitable neurons cannot use their power and fail to efficiently dictate the rhythm to the network. So, it seems that only a fine-tuned ratio between long- and short-range connections ensures the greatest collective coherence of noise-induced spikes. In such a network, neurons with the highest excitability operate as hubs that drive the dynamics of a local interconnected neighborhood (see middle column in Fig. 1) and besides communicate among themselves with long-range links.

We additionally examined the role of scaling exponent β, which characterizes the distribution of excitability [see Eq. (3)]. In particular, we verified if qualitatively similar results are obtained for different values of β. Results are shown in Fig. 4. A comparison to Fig. 2 reveals that for other values of β, comparable results are obtained, since in all cases an intermediate network configuration exists at which the greatest coherence is achieved. However, for lower values of the scaling exponent (β=1.5 and β=2), the optimal response is attained at higher values of δ, whereas for β=3 and β=3.5, the optimum is located at lower values of δ. In other words,

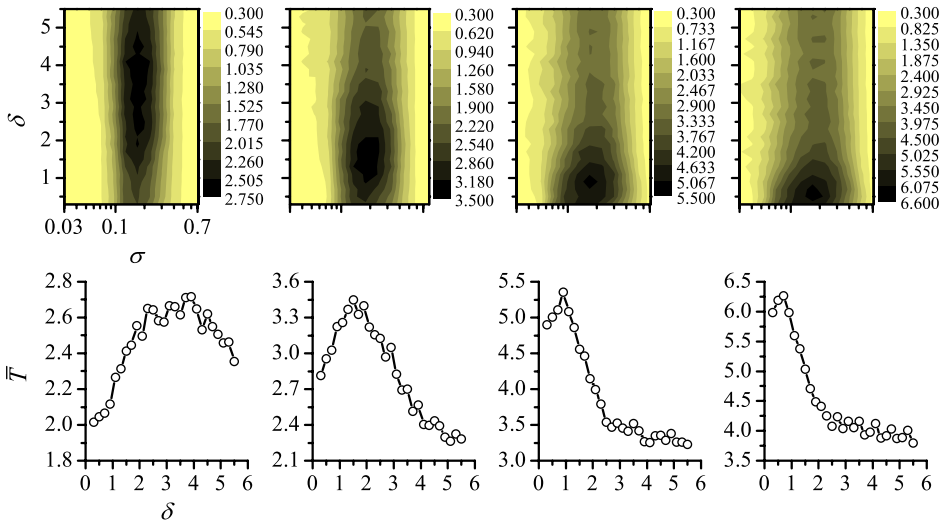

FIG. 4. (Color online) Color-coded values of $\bar{T}$ in dependence on σ and δ (upper row) and the cross section of the color map at optimal noise intensity σ=0.17 (lower row) for different scaling exponents: β=1.5 (left column), β=2 (second column from left), β=3 (third column from left), and β=3.5 (right column).

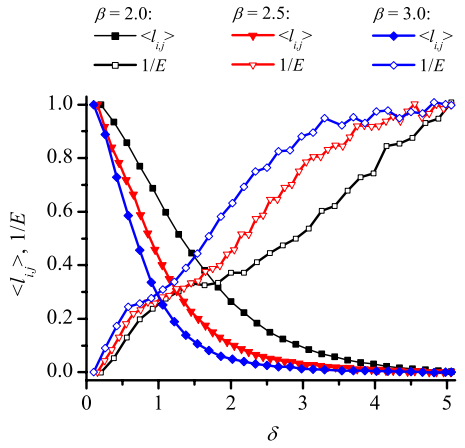

FIG. 5. (Color online) Normalized average Euclidian distance between coupled units $\langle l_{i,j} \rangle$ and the mean path length quantified via $1/E$ in dependence on δ for different scaling exponent values β.

there is a shift of the optimal network configuration toward lower values of δ as β is increased. This phenomenon is further analyzed in the continuation.

To establish a link between the dynamics and the structure of the network, we calculate the global efficiency of the network and the average Euclidean distance between the edges in dependence on the network parameter δ. The average Euclidean distance $\langle l_{i,j} \rangle$ is simply calculated by averaging all the distances $l_{i,j}$ between the units which are connected with each other. The efficiency E, an indicator of the traffic capacity of the network, is defined as follows:

$$E = \frac{1}{N(N-1)} \sum_{i \neq j} \frac{1}{d_{i,j}}, \tag{8}$$

where $d_{i,j}$ is the length of the geodesic from unit i to unit j. It can be noticed that E is inversely related to the average minimum path length, but is numerically easier to use for the estimation of topological distances between elements of disconnected graphs.

Since we are actually interested in comparison of the average geodesic distance dependence on the network structure and how the average Euclidean distance changes when δ is varied, we analyze the $1/E$ and $\langle l_{i,j} \rangle$ dependence on δ. In this way, we seek to quantify the crossover from a heterogeneous to a homogeneous network organization. For a better comparison, we normalized both quantities, $1/E$ and $\langle l_{i,j} \rangle$, so that they are bounded in the unit interval. Results for three different values of the scaling exponent β are shown in Fig. 5. As it has been qualitatively ascertained in Fig. 1, $\langle l_{i,j} \rangle$ decreases as δ is increased, whereas the average shortest path length, quantified via $1/E$, is increasing. Most remarkably, for all three values of β, the curves intersect at approximately the same values of δ which were identified to warrant the optimal response of the system (see Figs. 2 and 4). We can thus hypothesize that the points of intersection designate the turning point between a network with mainly long-range connections and a network where principally only short-range connections exist. We notice that for higher values of the scaling exponent β, the crossover is inferred at lower values of δ. This observation is completely in accordance with the results shown in Fig. 4, where the optimal δ is also found decreasing as β is increased.

IV. DISCUSSION

We studied the coherence resonance phenomenon on a spatially embedded vertex fitness network model. By smoothly varying the network topology from a scale-free-like to a topology that exhibits random geometric graph properties, we found that besides optimal noise intensity, also an intermediate network configuration exists, at which the noise-induced oscillations are the most regular. For various distributions of excitability, the optimal topology always lies between a scale-free network organization with dominating long-range connections and a network with a strong geometric regime. In particular, the greatest response of the network is achieved if both, long-range as well as short-range connections are present. In this case, some excitable units act as hubs that govern the dynamics of a local interconnected neighborhood. Moreover, there are some long-range links in the network, which principally represent connections between those hubs (see middle column in Fig. 1). For comparison, hubs are also present in scale-free networks; however, in this case, the hubs act as global pacemakers with a very large node degree influencing very different parts of the network, which does not ensure such a coherent response of the whole network. On the other hand, in case of regular geometric networks, where hubs are missing, a global coherent response of the network is also hard to obtain. Therefore, an optimal number of hubs and optimal ration between short- and long-range connections are required.

Although the results are obtained for a rather simple network representation of a neural architecture, they allow us to discuss several interesting aspects of possible functional organization and topology of complex neural networks. Two of them are of particular importance. First, the neural network organization can neither be firmly described by a regular network nor it can be treated as a pure scale-free network; however, the network must at least contain a few "hub" neurons possessing long-range connections that link large numbers of cells. Second, the variability of neurons is of crucial importance for optimal stochastic resonant responses.

The existence of hub neurons is still speculative. Graph theory predicts that topologies, which include hubs, represent an effective design to orchestrate synchronization and, in general, offer a compromise between computational needs, wiring economy, and robustness. The usual understanding of such networks is that the neurons are mostly connected with their neighbors, but also connected by some long-range links [20]. For archetypal anatomical neural networks, for example, it is known that on one hand, they have a degree distribution compatible with the existence of hubs, but on the other hand, they are sparsely connected, so that the physical distance between neurons is close to minimal [19]. In that way, an efficient information transport between nodes is achieved at low connectivity cost. A closer inspection of the results presented in Fig. 5 reveals that these circumstances can be regarded as fulfilled in the proximity of the critical

points. Namely, even if the mean path length is larger at optimal network configuration and with that the global efficiency is lower, the average Euclidean distance between neurons is at that point much lower than in case the average geodesic distance is minimal. Apparently, the optimal ratio between those quantities is attained in the vicinity of points of intersection.

Experimentally, the existence of neuronal hubs is hard to confirm, perhaps of the conceptual and technical difficulties of investigating them, including the rarity of high-connected cells (hubs) as compared to all other low-connected cells. However, recently, a considerable progress in experimental investigations has been made. A method was designed to map functional connectivity in real time in living brain slices, which confirmed the existence of functional hubs and helped to find cells involved in the synchronization of neuronal networks [29]. The most recent hypotheses indicate that the neuronal hubs orchestrate physiologically relevant activity in cortical assemblies, as well as being causal in producing pathological oscillations [29,30].

The synchronization and phase locking are no longer directly and automatically related to only pathological behaviors such as epilepsy. It has been shown, for example, that exactly the phase-locked oscillating neuronal groups can interact effectively because their communication windows for input and for output are open at the same time. Thus, a flexible pattern of coherence defines a flexible structure, which subserves our cognitive flexibility [31].

The pathological behaviors are also not directly connected to a given network structure. In particular, for neuronal networks characterized by hubs, it has been shown that by changing parameters such as the synaptic strengths, number of synapses per neuron, and proportion of local versus long-distance connections, all kinds from "normal," "seizing," and "bursting" behaviors can be obtained [32]. In this context, the seizing phase is related to the second epileptic phase characterized by high-frequency oscillations, usually following after the first stage of depolarization [33].

Next, we emphasize the importance of neuron variability. We found that the variability of neurons is of crucial importance for optimal stochastic resonant responses. This model prediction is fully in accordance with very recent studies noting the importance of variability of units constituting the network, which is an apparent feature of several real-life systems including neurons [15,23,34]. These studies examine heterogeneity in neuronal systems, where the disparity between individual neurons is obvious [35] and has besides been realized to constructively affect the dynamic behavior of coupled neurons [36]. However, in order to be able to assess the real biological relevance of this model as well as to find the physiological origin of all the short-range and long-range links, additional experimental and theoretical studies will be needed in the future.

[1] L. Gammaitoni, P. Hänggi, P. Jung, and F. Marchesoni, Rev. Mod. Phys. **70**, 223 (1998); M. D. McDonnell and D. Abbott, PLOS Comput. Biol. **5**, e1000348 (2009).

[2] H. Gang, T. Ditzinger, C. Z. Ning, and H. Haken, Phys. Rev. Lett. **71**, 807 (1993).

[3] A. S. Pikovsky and J. Kurths, Phys. Rev. Lett. **78**, 775 (1997).

[4] B. Lindner, J. García-Ojalvo, A. Neiman, and L. Schimansky-Geier, Phys. Rep. **392**, 321 (2004); X. Li, J. Wang, and W. Hu, Phys. Rev. E **76**, 041902 (2007); V. Volman and H. Levine, Phys. Rev. E **77**, 060903(R) (2008); Y. Chen, L. Yu, and S.-M. Qin, *ibid.* **78**, 051909 (2008); D. Guo and C. Li, *ibid.* **79**, 051921 (2009).

[5] M. C. Cross and P. C. Hohenberg, Rev. Mod. Phys. **65**, 851 (1993).

[6] F. Moss and K. Wiesenfeld, Sci. Am. **273**, 66 (1995).

[7] Y. Nagai, H. González, A. Shrier, and L. Glass, Phys. Rev. Lett. **84**, 4248 (2000).

[8] S. Kádár, J. Wang, and K. Showalter, Nature (London) **391**, 770 (1998).

[9] M. Giudici, C. Green, G. Giacomelli, U. Nespolo, and J. R. Tredicce, Phys. Rev. E **55**, 6414 (1997).

[10] H. Malchow, F. M. Hilker, R. R. Sarkar, and K. Brauer, Math. Comput. Modell. **42**, 1035 (2005).

[11] F. Sagués, J. M. Sancho, and J. García-Ojalvo, Rev. Mod. Phys. **79**, 829 (2007).

[12] C. J. Tessone, C. R. Mirasso, R. Toral, and J. D. Gunton, Phys. Rev. Lett. **97**, 194101 (2006).

[13] M. Perc, M. Gosak, and S. Kralj, Soft Matter **4**, 1861 (2008).

[14] H. Chen, J. Zhang, and J. Liu, Phys. Rev. E **75**, 041910 (2007); M. Gosak, Biophys. Chem. **139**, 53 (2009).

[15] E. Glatt, M. Gassel, and F. Kaiser, Phys. Rev. E **75**, 026206 (2007); C. J. Tessone, A. Scirè, R. Toral, and P. Colet, *ibid.* **75**, 016203 (2007); E. Glatt, M. Gassel, and F. Kaiser, Europhys. Lett. **81**, 40004 (2008); H. Chen, J. Zhang, and J. Liu, Physica A **387**, 1071 (2008).

[16] D. J. Watts and S. H. Strogatz, Nature (London) **393**, 440 (1998); R. Albert and A.-L. Barabási, Rev. Mod. Phys. **74**, 47 (2002); A.-L. Barabási, Science **325**, 412 (2009).

[17] S. Wasserman and K. Faust, *Social Network Analysis* (Cambridge University Press, Cambridge, England, 1994); L. A. Adamic, B. A. Huberman, A.-L. Barabási, R. Albert, H. Jeong, and G. Bianconi, Science **287**, 2115 (2000); M. E. J. Newman, Proc. Natl. Acad. Sci. U.S.A. **98**, 404 (2001); A.-L. Barabási and Z. N. Oltvai, Nat. Rev. Genet. **5**, 101 (2004).

[18] S.-H. Yook, H. Jeong, and A.-L. Barabási, Proc. Natl. Acad. Sci. U.S.A. **99**, 13382 (2002); K. Xu, X. Hong, and M. Gerla, J. Parallel Distrib. Comput. **63**, 110 (2003); H. Yang, Y. Nie, H. Zhang, Z. Di, and Y. Fan, Comput. Phys. Commun. **180**, 1511 (2009).

[19] C. C. Hilgetag, G. A. Burns, M. A. O'Neill, J. W. Scanell, and M. P. Young, Philos. Trans. R. Soc. London, Ser. B **355**, 91 (2000); O. Sporns, D. R. Chialvo, M. Kaiser, and C. C. Hilgetag, Trends Cogn. Sci. **8**, 418 (2004); V. M. Eguíluz, D. R. Chialvo, G. A. Cecchi, M. Baliki, and A. V. Apkarian, Phys. Rev. Lett. **94**, 018102 (2005); C. Zhou, L. Zemanova, G. Zamora, C. C. Hilgetag, and J. Kurths, *ibid.* **97**, 238103

(2006); D. S. Bassett and E. Bullmore, Neuroscientist **12**, 512 (2006); E. Bullmore and O. Sporns, Nat. Rev. Neurosci. **10**, 186 (2009).
[20] G. Buzsáki, C. Geisler, D. A. Henze, and X.-J. Wang, Trends Neurosci. **27**, 186 (2004).
[21] Z. Gao, B. Hu, and G. Hu, Phys. Rev. E **65**, 016209 (2001); O. Kwon and H. T. Moon, Phys. Lett. A **298**, 319 (2002); M. Perc, Phys. Rev. E **76**, 066203 (2007); M. Ozer, M. Perc, and M. Uzuntarla, Phys. Lett. A **373**, 964 (2009); M. Ozer, M. Perc, M. Uzuntarla, Europhys. Lett. **86**, 40008 (2009).
[22] J. A. Acebrón, S. Lozano, and A. Arenas, Phys. Rev. Lett. **99**, 128701 (2007); Z. Liu and T. Munakata, Phys. Rev. E **78**, 046111 (2008); M. Perc, *ibid.* **78**, 036105 (2008); H. Chen, Y. Shen, Z. Hou, and H. Xin, Chaos **19**, 033122 (2009).
[23] X. Li, J. Zhang, and M. Small, Chaos **19**, 013126 (2009).
[24] G. Caldarelli, A. Capocci, P. De Los Rios, and M. A. Muñoz, Phys. Rev. Lett. **89**, 258702 (2002).
[25] V. D. P. Servedio, G. Calderelli, and P. Buttà, Phys. Rev. E **70**, 056126 (2004).
[26] S. Morita, Phys. Rev. E **73**, 035104(R) (2006).
[27] R. Fitzhugh, Biophys. J. **1**, 445 (1961); J. S. Nagumo, S. Arimoto, and S. Yoshizawa, Proc. IRE **50**, 2061 (1962); D. Barkley, M. Kness, and L. S. Tuckerman, Phys. Rev. A **42**, 2489 (1990).
[28] A. L. Hodgkin and A. F. Huxley, J. Physiol. **117**, 500 (1952).
[29] P. Bonifazi, M. Goldin, M. A. Picardo, I. Jorquera, A. Cattani, G. Bianconi, A. Represa, Y. Ben-Ari, and R. Cossart, Science **326**, 1419 (2009).
[30] E. V. Lubenov and A. G. Siapas, Nature (London) **459**, 534 (2009).
[31] P. Fries, Trends Cogn. Sci. **9**, 474 (2005).
[32] T. I. Netoff, R. Clewley, S. Arno, T. Keck, and J. A. White, J. Neurosci. **24**, 8075 (2004).
[33] C. Borck and J. G. Jefferys, J. Neurophysiol. **82**, 2130 (1999).
[34] C. A. S. Batista, A. M. Batista, J. A. C. de Pontes, R. L. Viana, and S. R. Lopes, Phys. Rev. E **76**, 016218 (2007); C.-S. Chen, H.-S. Chen, and J.-Q. Zhang, Chin. Phys. Lett. **25**, 1591 (2008).
[35] S. Bixby, G. M. Kruger, J. T. Mosher, N. M. Joseph, and S. J. Morrison, Neuron **35**, 643 (2002); T. Klausberger and P. Somogyi, Science **321**, 53 (2008).
[36] C. Zhou, J. Kurths, and B. Hu, Phys. Rev. Lett. **87**, 098101 (2001).